


Dynamical cluster size heterogeneity

Amanda de Azevedo-Lopes ¹, André R. de la Rocha,¹ Paulo Murilo C. de Oliveira,^{2,3} and Jeferson J. Arenzon ^{1,3,*}

¹*Instituto de Física, Universidade Federal do Rio Grande do Sul, CP 15051, 91501-970 Porto Alegre RS, Brazil*

²*Instituto de Física, Universidade Federal Fluminense, Av. Litorânea s/n, 24210-340 Boa Viagem, Niterói, RJ, Brazil*

³*Instituto Nacional de Ciência e Tecnologia–Sistemas Complexos, 22290-180 Rio de Janeiro RJ, Brazil*



(Received 28 October 2019; published 6 January 2020)

Only recently has the essential role of the percolation critical point been considered on the dynamical properties of connected regions of aligned spins (domains) after a sudden temperature quench. In equilibrium, it is possible to resolve the contribution to criticality by the thermal and percolative effects (on finite lattices, while in the thermodynamic limit they merge at a single critical temperature) by studying the cluster size heterogeneity, $H_{\text{eq}}(T)$, a measure of how different the domains are in size. We extend this equilibrium measure here and study its temporal evolution, $H(t)$, after driving the system out of equilibrium by a sudden quench in temperature. We show that this single parameter is able to detect and well-separate the different time regimes, related to the two timescales in the problem, namely the short percolative and the long coarsening one.

DOI: [10.1103/PhysRevE.101.012108](https://doi.org/10.1103/PhysRevE.101.012108)

I. INTRODUCTION

The ferromagnetic Ising model displays relatively homogeneous configurations when equilibrated either at temperatures $T \ll T_c$ or $T \gg T_c$, where T_c is its critical temperature. In the former case, thermal fluctuations in the giant, equilibrium background cluster of aligned spins are energetically inhibited but increase in probability with temperature. In the opposite limit, well above T_c , large domains of parallel spins are unstable against the thermal noise, which breaks them into small clusters whose average size decreases with temperature. At these extreme limits, the size diversity is smaller than that found close to T_c , where the distribution of allowed sizes is very broad, with a fully developed power law (in the thermodynamic limit, $L \rightarrow \infty$). Because neighboring parallel spins are not necessarily correlated, besides the geometric clusters described above, Coniglio-Klein (CK) clusters [1] may be built by removing a temperature-dependent fraction of the parallel pairs from the geometric clusters. These so called physical clusters have been useful in developing powerful simulation algorithms [2,3] and to unveil geometric properties for both models and experimental systems [4–9] that characterize both the equilibrium critical behavior [1,10] and the out-of-equilibrium dynamics [4]. The domain size distribution only becomes dense in the infinite-size limit or after ensemble averages are taken, while for a single, finite sample, space constraints forbid the presence of every possible cluster size, and the distribution gets truncated and sparse, subject to sample-to-sample fluctuations. A simple, global measure of the heterogeneity of a finite equilibrium configuration was introduced [11–15], only taking into account whether a given size is present in a configuration. The cluster size heterogeneity (H) is defined as the number of distinct cluster sizes,

irrespective of the number of equally sized domains, that are present in a finite-size sample.

The results for the equilibrium cluster size heterogeneity $H_{\text{eq}}(T)$ of the geometrical domains in the two-dimensional (2D) Ising model show a double peak structure at two very distinct temperatures. The small peak at $T_1 \simeq T_c$, associated with the thermal transition [14], is only observed for sufficiently large systems [15]. The peak grows as $H_{\text{eq}}(T_1) \sim L^{d/\tau}$, where $\tau = 379/187 \simeq 2.027$ is the Fisher exponent associated with the power-law cluster size distribution at the critical temperature of the Ising model [16,17]. In spite of the thermal and percolative transitions occurring at the same T_c , for finite systems these effects have not yet merged. Indeed, the percolative contribution appears as a second, much larger peak [15], at a temperature significantly higher than T_c [e.g., $T_2(L) \simeq 2T_c$ for $L = 640$]. The height of this second peak behaves as $H_{\text{eq}}(T_2) \sim L^{d/\tau'(L)}$. The exponent τ' , associated with the height of the second peak, is closer to the percolation value, $\tau_p = 187/91 \simeq 2.055$, but it should cross over to τ as the two peaks merge in the thermodynamic limit. The double-peaked heterogeneity is a property of the geometric domains, while the physical (CK) domains, on the other hand, have a single peak similar to the susceptibility. Thus, for equilibrium finite samples, when describing the thermal and percolation transitions with the cluster heterogeneity of geometric domains, they seem to be disentangled, each one affecting the geometric properties more effectively at different temperatures (where the peaks are located), suggesting that the corresponding mechanisms may be different. The smaller the system is, the larger is the interval between these peaks. Whether this equilibrium separation translates to a temporal resolution is an interesting question. Thus, the main objective of this paper is to explore whether this measure may be useful to study not only equilibrium properties of simple models but their dynamics as well.

After a quench from infinite to a below-critical temperature, the out-of-equilibrium, single-flip dynamics of the

*arenzon@if.ufrgs.br

nonconserved order parameter 2D Ising model is first attracted by the percolative critical point and only then crosses over to the coarsening regime [18,19]. In the process, a percolation cluster first appears in the early stages (t_p) of the dynamics [18,19], but it only becomes stable on a longer, size-dependent timescale $t_p \sim L^{z_p}$ [20,21] where the exponent has been conjectured to be $z_p = 2/5$ [21] for the square lattice. This initially percolating cluster strongly correlates with the asymptotic state [20,22–28]. The domain growth eventually leads to the fully magnetized ground state for roughly 2/3 of the random initial configurations. The second most frequent outcome is a configuration of parallel stripes, while diagonal stripes have a much smaller probability (and a longer timescale). During the evolution, as the domains keep decreasing the excess energy at the curved interfaces, there appears a growing characteristic length associated with the coarsening regime, $\ell_d(t) \sim t^{1/z_d}$, with $z_d = 2$ [4].

The existence of a characteristic length obviously does not imply that the system is homogeneous, with domains similarly sized. A possible measure of the diversity of the actual sizes is the cluster size heterogeneity previously discussed, extended here to out-of-equilibrium configurations. While both the initial and the asymptotic equilibrium values of H_{eq} have been measured [15], there are many questions related to the intermediate time evolution of $H(t)$. In particular, since H_{eq} seems very responsive to the percolative equilibrium properties, does the dynamical size heterogeneity give information on the two regimes, approaching and departing from the critical percolation point, before the dynamics is dominated by coarsening? How distinct are these regimes? Is $H(t)$ monotonic in time or is there one or two peaks related to the equilibrium behavior? Is it possible for a single parameter to give information on the two length scales associated with coarsening? How do different initial and final temperatures change the behavior? We address some of these questions, showing that the dynamical cluster size heterogeneity, $H(t)$, is indeed a suitable observable that not only distinguishes among different dynamical regimes, but also provides quantitative access to the scaling laws related to the growth of correlations and of percolative clusters during the dynamics. Furthermore, we show that the time evolution of $H(t)$ correlates with the nature of the correlations present in the initial state, whether long-range if the quench is performed from $T_0 = T_c$, or absent from $T_0 \rightarrow \infty$. It is also noteworthy that the short-time regime of $H(t)$ resulting from the dynamics triggered from $T_0 \rightarrow \infty$ to $T = 0$ allows a quantitative connection with the percolation-related peak observed in the equilibrium heterogeneity, $H_{\text{eq}}(T_2)$.

II. DYNAMICAL CLUSTER HETEROGENEITY

Following different temperature quench protocols that drive the system out of equilibrium, we study the 2D Ising model whose Hamiltonian is

$$\mathcal{H} = -J \sum_{(ij)} \sigma_i \sigma_j, \quad (1)$$

where $J > 0$, $\sigma_i = \pm 1$ is the spin at site i , and the sum is over all nearest-neighbor sites on an $L \times L$ square lattice with periodic boundary conditions (L is measured in units of the

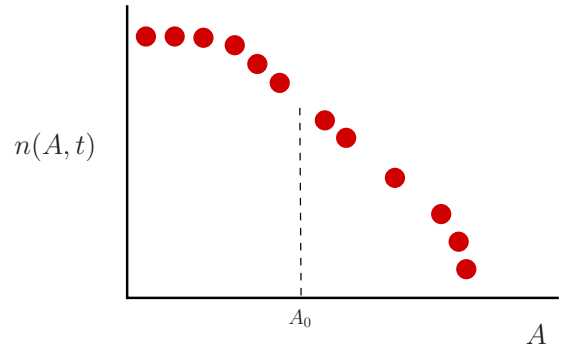


FIG. 1. Schematic cluster size distribution for a single, finite sample. Differently from an infinite system or averaged distribution, some sizes have no realizations. The smallest missing size, A_0 , is indicated by a vertical dashed line, separating the dense region of the distribution, $A < A_0$, from the sparse one, $A > A_0$. Those sizes that are indeed present in the specific configuration define a measure of the cluster size heterogeneity (in this example, $H = 12$).

lattice spacing ℓ_0). We choose the initial temperature T_0 to be either infinite or the critical one, these equilibrium states thus differing by having zero or infinite range correlations, respectively. The fixed temperature adopted after the quench is $T = 0$. The simulations were performed on square lattices with linear sizes up to $L = 5120$. Averages up to 1000 samples were taken for the smaller systems, while larger sizes require fewer samples (100). When $T_0 = T_c$ it is necessary to equilibrate the system, and 1000 Swendsen-Wang steps were performed, while during the subsequent temporal dynamics, in all cases, a fast version of the single-spin Glauber algorithm at $T = 0$ was used [29]. Time is measured in Monte Carlo steps (MCSs), where one unit corresponds to N attempts to flip.

Along the time evolution of the system, we measure the dynamical cluster size heterogeneity $H(t)$, taking into account only the nonspanning clusters [the presence of one or more spanning clusters does not have a large influence on $H(t)$, except close to the asymptotic state, where it is small]. It is defined, as in the equilibrium case, as the number of different cluster sizes present at time t on a finite-size configuration (see the schematic depiction in Fig. 1). Although different domain definitions are possible, we consider here only geometrical domains, i.e., sets of connected parallel spins.

A. Quench from T_c to $T_f = 0$

After a quench from the equilibrium initial state at the Ising critical temperature ($T_0 = T_c$), the cluster size distribution of geometric domains evolves as [18,19]

$$n(A, t) \simeq \frac{c[\lambda(t+t')]^{\tau-2}}{[A + \lambda(t+t')]^{\tau}}, \quad (2)$$

where $n(A, t)dA$ is the average number of (nonspanning) clusters, per unit area, whose size is between A and $A + dA$. The constant $c \simeq 0.029$ [18,19] is very close to the Cardy-Ziff number [10], $c_h = 1/(8\pi\sqrt{3}) \simeq 0.023$, $\lambda \simeq 2$ (time and area units are unitary) is a temperature-dependent material constant (the chosen value is for $T = 0$), and t' is a microscopic

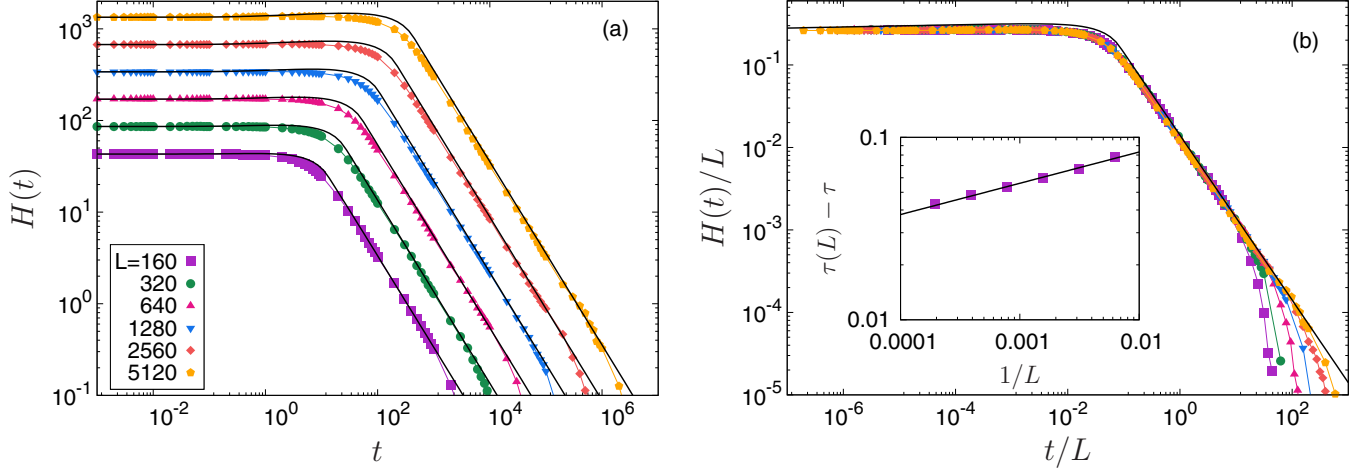


FIG. 2. Dynamical cluster size heterogeneity, $H(t)$, as a function of time (in MCS) after a temperature quench from $T_0 = T_c$ down to $T_f = 0$. For simplicity, only those samples that converged to a fully magnetized state were considered. (a) In the first regime, $t \leq t_0$, $H(t)$ presents a slow variation starting from $H_{\text{eq}}(T_c)$, Eq. (7), while in the power-law regime, the behavior is t^{-1} . The whole behavior is well approximated by Eq. (6) and shown as solid lines. We consider $c \simeq 0.029$, $\lambda \simeq 2$, and τ to take finite-size effects into account, as a fitting parameter. (b) The simulation data collapse well onto a universal curve, $H(t) = Lf(t/L)$, using the asymptotic value of the Fisher exponent, $\tau = 379/187$. The agreement with Eq. (6) is also very good. The inset shows that the values of $\tau(L)$ that better fit the data in panel (a) do converge to the correct value as L increases.

time such that $\lambda t' \simeq 1$. The above distribution is an average while the heterogeneity H is measured from single configurations as schematically shown in Fig. 1. At the moment of the quench, there is an already stable spanning cluster, $t_p \simeq t_{p_1} \simeq 0$ [20]. Differently from the averaged distribution of Eq. (2), for a single sample there are holes in the distribution, as not all possible sizes may be present. Denoting by $A_0(t)$ the smallest missing size at time t , the sample cluster size distribution is dense for $A < A_0(t)$ and sparse above it. If ℓ_0 is a microscopic length and $(\ell_0 L)^2$ is the area of the system, A_0 is the size such that $(L\ell_0)^2 n(A_0, t) \ell_0^2 \sim 1$. Thus, setting $\ell_0 = 1$, we obtain that

$$A_0(t) \simeq (\lambda t + 1) \left[\left(\frac{L\sqrt{c}}{\lambda t + 1} \right)^{2/\tau} - 1 \right] \Theta(t - t_0) \quad (3)$$

and the dense region of the cluster size distribution, on average, disappears after a time

$$t_0 \simeq \frac{L\sqrt{c}}{\lambda}. \quad (4)$$

The cluster size heterogeneity after the quench, $H(t)$, is shown in Fig. 2(a) for different lattice sizes. The coarsening process moves the whole distribution to the left, removing the smallest clusters, initially changing very slowly the value of $H(t)$ up to $t \simeq t_0$. It then crosses over to a different regime, decreasing as a power law, when the dense region is about to disappear. Once the remaining distribution is sparse, almost all present cluster sizes appear only once, and $H(t)$ becomes equivalent to the number of clusters. These two contributions to $H(t)$ may be approximated by

$$H(t) \simeq A_0 + L^2 \int_{A_0}^{\infty} dA n(A, t), \quad (5)$$

where the first and second terms correspond, respectively, to the size of the dense region and the number of clusters in the sparse one. Using Eqs. (2) and (3) with Eq. (5), we get an

expression for $H(t)$ at all times:

$$H(t) \simeq \begin{cases} (\lambda t + 1) \left[\frac{\tau}{\tau - 1} \left(\frac{L\sqrt{c}}{\lambda t + 1} \right)^{2/\tau} - 1 \right], & t \leq t_0, \\ \frac{L^2 c}{\tau - 1} \frac{1}{\lambda t + 1}, & t \geq t_0. \end{cases} \quad (6)$$

Notice that $H(t \rightarrow \infty) = 0$ in the above expression because, in our definition, the spanning clusters are not accounted for. At $t = t_0 \simeq L\sqrt{c}/\lambda$, both terms give $H(t_0) \simeq L\sqrt{c}/(\tau - 1)$ while the initial value, corresponding to the equilibrium state at T_c , is

$$H(0) \simeq H_{\text{eq}}(T_c) \simeq \frac{\tau}{\tau - 1} c^{1/\tau} L^{2/\tau}. \quad (7)$$

Figure 2(a) also compares the simulations with the above expression for $H(t)$ as solid lines. The agreement is pretty good, except where there is a change of regime, close to t_0 , where $n(A, t)$ is still significant and there may be more than one cluster with the same size, originating the small deviation seen in Figs. 2(a) and 3. Despite its exact value being known, we have considered τ as a fitting parameter in order to take finite-size effects into account. The inset of Fig. 2(b) shows the values of $\tau(L)$ obtained from each fit (performed only for the initial times, $t < 10^{-2}$) and how they converge to $\tau = 379/187$ as $L \rightarrow \infty$. Figure 2(b) also shows that the same data, when properly rescaled, present an excellent collapse. From Eq. (6) we see that the rescaling is $H(t) = L^{-1} f(t/L)$, where $f(x) \sim x^{-1}$ (a power-law decay) for $x \gg 1$, and $x^{1-2/\tau}$ (a very slow increase) for $x \ll 1$. There is a further, subtle feature of the numerical data, again well captured by Eq. (6), that can be seen in Fig. 3: $H(t)$ is not a monotonous function. It presents a maximum $H(t_{\text{max}})$ whose location agrees well with the numerical data,

$$\frac{\lambda t_{\text{max}} + 1}{L} = \sqrt{c} \left(\frac{\tau - 2}{\tau - 1} \right)^{\tau/2} \simeq 0.004, \quad (8)$$

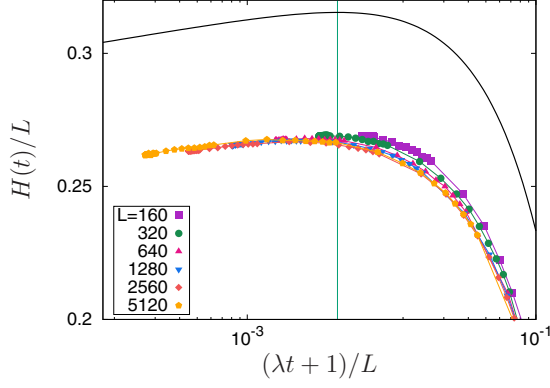


FIG. 3. Zoom into the region close to the end of the plateau, after a quench from $T_0 = T_c$, showing a very small peak at t_{\max} (vertical line), Eq. (8). The height of the peak in Eq. (6) depends on the precise value of c , and the difference from the numerical data appears larger because of the chosen scale.

although the height has a small deviation (enlarged in Fig. 3 because of the chosen vertical scale).

B. Quench from $T_0 \rightarrow \infty$ to $T_f = 0$

When quenching the system from $T_0 \rightarrow \infty$ down to $T_f = 0$, the general cluster size heterogeneity behavior can be seen in Fig. 4(a). At the initial high temperature, despite spins being uncorrelated, small clusters of parallel spins are present. The initial heterogeneity is not very large and slowly grows with the system size, $H_{\text{eq}}(T \rightarrow \infty) \sim \ln L$ [12,14,15], as can be observed in Fig. 4(a). Soon after the quench, $H(t)$ presents a pronounced peak followed by a growing, intermediate plateau before the final power-law decrease toward the asymptotic

state. The dynamics is eventually attracted [22,24,25,27] to a state that is either fully magnetized or contains on- or off-axis stripes. Although the results are similar, for simplicity we kept only those samples that got, eventually, fully magnetized.

Differently from the previous case, the initial equilibrium state at $T_0 \rightarrow \infty$ is not critical. Nonetheless, before entering the scaling regime, the system first approaches the random site percolation critical state [18,19], with an average cluster size distribution given by a power law $A^{-\tau_p}$ whose Fisher exponent is $\tau_p = 187/91$. As discussed in the Introduction, the first occurrence of a percolating, albeit unstable, cluster is at the early time t_{p_1} , while at t_p it becomes stable. After the cluster size distribution becomes critical at t_{p_1} , its time evolution is well approximated by [18,19,21]

$$n(A, t) \simeq \frac{2c[\lambda(t + t_{p_1} + t')]^{\tau_p - 2}}{[A + \lambda(t + t_{p_1} + t')]^{\tau_p}}, \quad (9)$$

where the factor 2 in the numerator comes from the existence of clusters with both positive and negative magnetizations, while in the related percolation problem only particle clusters, not voids, are accounted for. In analogy to the previous case, the behavior of $H(t)$ after a quench from $T_0 \rightarrow \infty$, calculated using Eq. (5), is given by

$$H(t) \simeq \begin{cases} (\lambda t + 1) \left[\frac{\tau_p}{\tau_p - 1} \left(\frac{L\sqrt{2c}}{\lambda t + 1} \right)^{2/\tau_p} - 1 \right], & t_{p_1} < t \leq t_0, \\ \frac{2L^2 c}{\tau_p - 1} \frac{1}{\lambda t + 1}, & t \geq t_0, \end{cases} \quad (10)$$

where, in this case, $t_0 \simeq L\sqrt{2c}/\lambda$. As in the $T_0 = T_c$ case, $H(t)$ also has a broad and small maximum before t_0 , more precisely at $(\lambda t_{\max} + 1)/L = \sqrt{2c}[(\tau_p - 2)/(\tau_p - 1)]^{\tau_p/2} \simeq 0.011$. However, this maximum does not appear in the simulation, and $H(t)$ seems to always decrease. This is

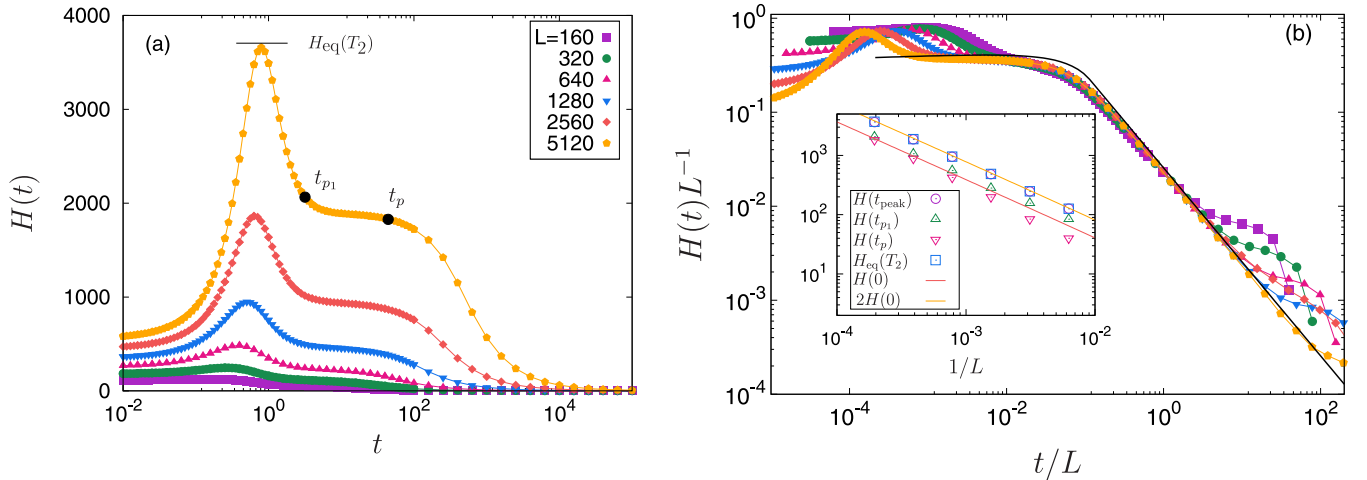


FIG. 4. (a) Dynamical cluster size heterogeneity $H(t)$ as a function of time (in MCS) after a temperature quench from $T_0 \rightarrow \infty$ down to $T_f = 0$. For simplicity, only those samples that converged to a fully magnetized state were considered. For the largest size, we indicate the times when a percolating cluster first appears and when it becomes stable, t_{p_1} and t_p , respectively. In Ref. [15] it was observed that the equilibrium heterogeneity, H_{eq} , has a second, larger peak at $T_2(L)$, well above $T_1 \simeq T_c$ where another, smaller peak is located. The value of $H_{\text{eq}}(T_2)$ agrees well with $H(t_{\text{peak}})$ and is shown, for the largest simulated size only, as a small horizontal line on top of the peak. (b) Data collapse. As the system size increases, a region between t_{p_1} and t_p , where $H(t)$ slowly changes, becomes apparent. The behavior for $t > t_{p_1}$ is well approximated by Eq. (10) with $\tau_p = 187/91$ (solid line). The inset shows, in the upper straight line, the height of the peaks $H(t_{\text{peak}})$ and $H_{\text{eq}}(T_2)$, indistinguishable at this scale, along with Eq. (12), as a function of the system size. The data below (triangles) correspond to the values of $H(t_p)$ and $H(t_{p_1})$ that, albeit different, get close as L increases.

because, for the sizes considered here, the region $t \leq t_0$ may not yet be fully developed, or it may be because of the presence of the initial, precursor maximum that reverses the behavior below t_{p_1} .

Since Eq. (9) considers an effective initial state at the percolation threshold, the above expression for $H(t)$ is not expected to capture any feature before t_{p_1} . Indeed, $t = 0$ corresponds to the beginning of the slowly changing region, which roughly extends between t_{p_1} and t_p (and whose width depends on L), observed in Figs. 4(a) and 4(b):

$$H(0) \simeq \frac{\tau_p}{\tau_p - 1} (L\sqrt{2c})^{2/\tau_p}. \quad (11)$$

In contrast with the $T_0 = T_c$ case, $H(t)$ has a very pronounced peak just before the appearance of the first percolating cluster, i.e., $t_{\text{peak}} < t_{p_1}$, which is a precursor feature of the percolating state. After the quench, as the correlations build larger clusters, the size distribution widens and $H(t)$ increases. However, as the largest cluster increases, less space remains for the other clusters. Thus, a state of maximum heterogeneity occurs slightly before t_{p_1} and the associated percolation transition. In particular, the height of the peak seems to correspond to the equilibrium heterogeneity at the second peak observed in Ref. [15], i.e., for each system size, $H(t_{\text{peak}}) \simeq H_{\text{eq}}(T_2)$, as indicated by a small horizontal line in Fig. 4(a) (only for the largest L). Moreover, we numerically observe that it is twice the height at t_{p_1} :

$$H(t_{\text{peak}}) \simeq H_{\text{eq}}(T_2) \simeq 2H(0) \simeq \frac{2\tau_p}{\tau_p - 1} (L\sqrt{2c})^{2/\tau_p}. \quad (12)$$

For $t \geq t_0$, the power-law behavior of $H(t)$ is similar to the $T_0 = T_c$ case and accounts for the number of clusters, differing only by the value of τ_p and the factor 2 in the numerator. The data for $t > t_{p_1}$ are well described by Eq. (10), as can be seen in Fig. 4(b).

Nonetheless, by rescaling both $H(t)$ and time by L [Fig. 4(b)], although the finite-size effects are somewhat stronger than in the $T_0 = T_c$ case, both the agreement with Eq. (10) and the collapse in the same region are very good.

Despite the strong, early peak being a precursor effect of the percolating cluster that appears soon afterward, $t_{\text{peak}} < t_{p_1}$, it has a strong connection with the equilibrium measures of Ref. [15]. Indeed, as the temperature is slowly decreased, the equilibrium peak at T_2 [15] also anticipates the first appearance of a percolating cluster. Interestingly, the data collapse in Fig. 4(b) fails in the very early regime, indicating that the dynamical scaling length $\xi(t) \sim t^{1/2}$ is not the sole relevant length scale after the quench. The precursor peak shifts to the left, indicating that a scaling factor L^α , with $\alpha < 1$, should be considered instead of L . Indeed, as seen in Fig. 5, a good collapse around the peak is obtained with $\alpha \simeq 0.22$. However, notice that although the peaks are well collapsed, neither the black circles indicating t_{p_1} nor the black squares for t_p present a good convergence. Different values of the exponent α can, on the other hand, collapse those characteristic times. For t_p , it was shown in Ref. [21] that the exponent is 0.4.

To check how universal the $H(t)$ behavior is, we compare in Fig. 6, for $L = 1280$, the behavior of $H(t)$ for the Ising model after a quench from $T_0 \rightarrow \infty$ and the Voter model (VM) evolving from a fully uncorrelated state. The VM is

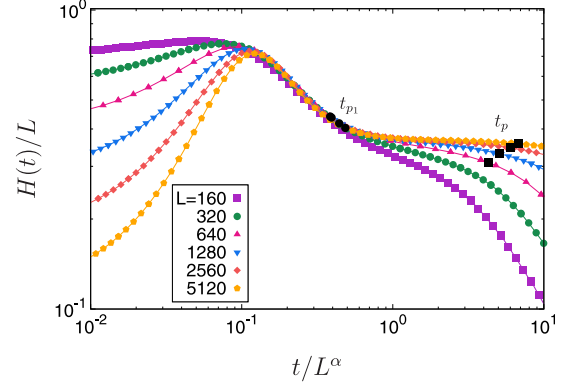


FIG. 5. Rescaling of the early time region near the peak of $H(t)$ after a temperature quench from $T_0 \rightarrow \infty$. The region that includes both the peak and t_{p_1} is well collapsed using $\alpha \simeq 0.22$.

interesting as there is no bulk noise, and detailed balance is not obeyed. Instead of considering the energy variation for a putative flip, as in the Ising model, in the VM the spin chooses and aligns with a single neighbor. As shown in Ref. [30], the timescales are all larger in the VM, nonetheless the overall behavior of $H(t)$ is similar, Fig. 6. Moreover, defining t_{p_1} and t_p as above (even if the critical properties of the percolating cluster do not correspond to critical percolation [30]), we can see in Fig. 6 that they are related, respectively, to the end of the precursor peak and the end of the plateau. A remarkable feature in this figure is the height of the early peak, which is roughly the same in both models, suggesting a more general mechanism.

III. CONCLUSIONS

In equilibrium at high temperatures, domains of parallel neighboring spins are not large and within a limited range of sizes, thus the number of different domain sizes in a given configuration, $H_{\text{eq}}(T)$, is small. Decreasing the temperature, spins become more correlated and the clusters increase and

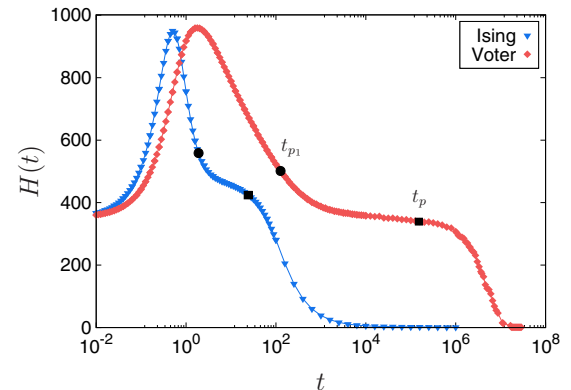


FIG. 6. Comparison between the time evolution of $H(t)$ for the Ising at $T = 0$ and the Voter model, both starting from an initially uncorrelated state ($T_0 \rightarrow \infty$). The system linear size is $L = 1280$ and time is in MCS. Notice that the precursor peak has roughly the same height for the two models, suggesting a common mechanism.

diversify, increasing H_{eq} . However, as some clusters get comparable to the size of the system, the lack of space tends to decrease the diversity. In the presence of these competing mechanisms, one expects a peak in H_{eq} . Remarkably, for geometric domains, two peaks are present [15], one near the temperature where the percolating cluster first appears [31] and a second one very close to T_c . We extended here this equilibrium measure of how heterogeneous the domains are in size to nonequilibrium situations, $H(t)$. Specifically, we explore its usefulness in the nonconserved order-parameter dynamics of the 2D Ising model after a sudden quench in temperature, confirming that this observable unveils the rich interplay between percolation and ferromagnetism either close to the phase transition (equilibrium) or at short-time scales during the dynamics.

For quenches starting at T_c , $H(t)$ presents an initial plateau that increases very slowly, attaining a shallow maximum before crossing over to a power-law behavior. In this latter regime, the sample size distribution is very sparse and the probability of two domains having the same size is small. The heterogeneity does correspond, in this time regime, to the total number of clusters and decays as a power law. When the system, instead, is first equilibrated at $T_0 \rightarrow \infty$ (random spin configuration), in addition to these regimes *after* it passes through the percolation critical point, there is also a very pronounced peak that is a precursor indication that a giant, percolating cluster is being built.

The rich behavior of $H(t)$ suggests that it would be interesting to consider several extensions, both in equilibrium and after a quench in temperature. While for the Ising model

each domain has a single neighbor and its size decreases at the same, constant rate, for the ($q > 2$) Potts model domains may either decrease or increase as their time evolution, given by the von Neumann law, depends on their number of sides. The coarsening behavior is thus richer [32–34]. As a consequence, domains with the same area but a different number of sides have a larger probability of evolving into different sizes, increasing the heterogeneity. Such a mechanism, which breaks the degeneracy of areas depending on the number of sides, is absent in the Ising model. Another interesting case is the Ising model with conserved order parameter [30,35,36] or disorder [37–39]. Although we focused here on geometric domains, the heterogeneity associated with the Coniglio-Klein clusters [1] would also be of interest [15], along with the heterogeneity of perimeters. The dynamics of the 3D Ising model is more challenging [24,40,41], as multiple frozen percolating clusters coexist and, for sufficiently large systems, the ground state is never reached. In addition, the thermal and percolation transitions do not coincide. Finally, it would be important to verify our results in experimental setups [5,9].

ACKNOWLEDGMENTS

We are grateful to R. Almeida, F. Corberi, L. Cugliandolo, M. Picco, and H. Takeuchi for useful conversations and/or comments on the manuscript. The work was partially supported by the Brazilian agencies FAPERGS (19/2551-0000555-5), FAPERJ, CNPq (423283/2016 and 308927/2017), and CAPES (Finance Code 001).

-
- [1] A. Coniglio and W. Klein, *J. Phys. A* **13**, 2775 (1980).
 - [2] R. H. Swendsen and J.-S. Wang, *Phys. Rev. Lett.* **58**, 86 (1987).
 - [3] U. Wolff, *Phys. Rev. Lett.* **62**, 361 (1989).
 - [4] A. J. Bray, *Adv. Phys.* **43**, 357 (1994).
 - [5] A. Sicilia, J. J. Arenzon, I. Dierking, A. J. Bray, L. F. Cugliandolo, J. Martinez-Perdiguero, I. Alonso, and I. C. Pintre, *Phys. Rev. Lett.* **101**, 197801 (2008).
 - [6] M. Castro, R. Cuerno, M. M. Garcia-Hernandez, and L. Vazquez, *Phys. Rev. Lett.* **112**, 094103 (2014).
 - [7] G. B. Deepa and R. Pratibha, *Phys. Rev. E* **89**, 042504 (2014).
 - [8] P. N. Timonin, *Physica A* **527**, 121402 (2019).
 - [9] R. Almeida and K. A. Takeuchi (private communication).
 - [10] J. Cardy and R. M. Ziff, *J. Stat. Phys.* **110**, 1 (2003).
 - [11] H. K. Lee, B. J. Kim, and H. Park, *Phys. Rev. E* **84**, 020101(R) (2011).
 - [12] J. D. Noh, H. K. Lee, and H. Park, *Phys. Rev. E* **84**, 010101(R) (2011).
 - [13] J.-P. Lv, X. Yang, and Y. Deng, *Phys. Rev. E* **86**, 022105 (2012).
 - [14] W. S. Jo, S. D. Yi, S. K. Baek, and B. J. Kim, *Phys. Rev. E* **86**, 032103 (2012).
 - [15] A. R. de la Rocha, P. M. C. de Oliveira, and J. J. Arenzon, *Phys. Rev. E* **91**, 042113 (2015).
 - [16] A. L. Stella and C. Vanderzande, *Phys. Rev. Lett.* **62**, 1067 (1989).
 - [17] W. Janke and A. M. J. Schakel, *Phys. Rev. E* **71**, 036703 (2005).
 - [18] J. J. Arenzon, A. J. Bray, L. F. Cugliandolo, and A. Sicilia, *Phys. Rev. Lett.* **98**, 145701 (2007).
 - [19] A. Sicilia, J. J. Arenzon, A. J. Bray, and L. F. Cugliandolo, *Phys. Rev. E* **76**, 061116 (2007).
 - [20] T. Blanchard, F. Corberi, L. F. Cugliandolo, and M. Picco, *Europhys. Lett.* **106**, 66001 (2014).
 - [21] T. Blanchard, L. F. Cugliandolo, M. Picco, and A. Tartaglia, *J. Stat. Mech.* (2017) 113201.
 - [22] B. Derrida, P. M. C. de Oliveira, and D. Stauffer, *Physica A* **224**, 604 (1996).
 - [23] A. Lipowski, *Physica A* **268**, 6 (1999).
 - [24] V. Spirin, P. L. Krapivsky, and S. Redner, *Phys. Rev. E* **63**, 036118 (2001).
 - [25] V. Spirin, P. L. Krapivsky, and S. Redner, *Phys. Rev. E* **65**, 016119 (2001).
 - [26] K. Barros, P. L. Krapivsky, and S. Redner, *Phys. Rev. E* **80**, 040101(R) (2009).
 - [27] J. Olejarz, P. L. Krapivsky, and S. Redner, *Phys. Rev. Lett.* **109**, 195702 (2012).
 - [28] T. Blanchard and M. Picco, *Phys. Rev. E* **88**, 032131 (2013).
 - [29] M. Newman and G. Barkema, *Monte Carlo Methods in Statistical Physics* (Oxford University Press, New York, 1999).
 - [30] A. Tartaglia, L. F. Cugliandolo, and M. Picco, *J. Stat. Mech.* (2018) 083202.
 - [31] H. Ricateau, L. F. Cugliandolo, and M. Picco, *J. Stat. Mech.* (2018) 013201.

- [32] M. P. O. Loureiro, J. J. Arenzon, L. F. Cugliandolo, and A. Sicilia, *Phys. Rev. E* **81**, 021129 (2010).
- [33] M. P. O. Loureiro, J. J. Arenzon, and L. F. Cugliandolo, *Phys. Rev. E* **85**, 021135 (2012).
- [34] J. Denholm and S. Redner, *Phys. Rev. E* **99**, 062142 (2019).
- [35] A. Sicilia, Y. Sarrazin, J. J. Arenzon, A. J. Bray, and L. F. Cugliandolo, *Phys. Rev. E* **80**, 031121 (2009).
- [36] H. Takeuchi, Y. Mizuno, and K. Dehara, *Phys. Rev. A* **92**, 043608 (2015).
- [37] A. Sicilia, J. J. Arenzon, A. J. Bray, and L. F. Cugliandolo, *Europhys. Lett.* **82**, 10001 (2008).
- [38] F. Corberi, L. F. Cugliandolo, F. Insalata, and M. Picco, *Phys. Rev. E* **95**, 022101 (2017).
- [39] F. Corberi, L. F. Cugliandolo, F. Insalata, and M. Picco, *J. Stat. Mech.* (2019) 043203.
- [40] J. J. Arenzon, L. F. Cugliandolo, and M. Picco, *Phys. Rev. E* **91**, 032142 (2015).
- [41] N. Vadakkayil, S. Chakraborty, and S. K. Das, *J. Chem. Phys.* **150**, 054702 (2019).